Energy, Mines and Resources Canada | Énergie, Mines et Ressources Canada

CANMET

Canada Centre for Mineral and Energy Technology | Centre canadien de la technologie des minéraux et de l'énergie

CALIBRATION OF AC POTENTIAL DROP TECHNIQUE FOR SIZING OF FATIGUE CRACKS IN WELDED JOINTS

O. Vosikovsky*, M. Chaar** and R. Bouchard*
Engineering Physics Section

January 1987

MICROMEDIA

PHYSICAL METALLURGY RESEARCH LABORATORIES
REPORT PMRL 87-1(TR)

21 pp

88-02158/

PHYSICAL METALLURGY RESEARCH LABORATORIES
REPORT PMRL 87-1(TR)

CALIBRATION OF THE AC POTENTIAL DROP TECHNIQUE FOR SIZING OF FATIGUE CRACKS IN WELDED JOINTS

by

O. Vosikovsky*, M. Chaar** and R. Bouchard*

ABSTRACT

A computerized calibration procedure for multiprobe alternating current potential drop (ACPD) fatigue crack depth measurements in welded plate T-joints is described. The calibration is based on crack depth measurements of beach marks and it is designed to monitor the maximum depth of the largest fatigue crack initiated from the weld toe.

Accuracy of calibration is estimated as ±20% for cracks deeper than 3 mm, and about ±0.5 mm for shallower cracks.

---

*PMRL/CANMET.

**University of Ottawa.

LABORATOIRE DE RECHERCHE EN METALLURGIE PHYSIQUE

RAPPORT PMRL 87-1(TR)

CALIBRATION DE LA TECHNIQUE DE DIFFERENCE DE POTENTIEL EN COURANT ALTERNATIF POUR DIMENSIONNER LES FISSURES DE FATIGUE DANS LES JOINTS SOUDES.

par

O. Vosikovski*, M. Chaar** and R.Bouchard*

RESUME

La procédure de calibration par ordinateur de la technique de différence de potentiel en courant alternatif à multisondes, pour les joints soudés en T, est décrite. La calibration est basée sur les mesures de profondeur des lignes d'arrêt des fissures et est conçue pour évaluer la profondeur de la plus grande fissure de fatigue initiée dans le cordon de la soudure.

La précision de la calibration est estimée à ±20% pour les fissures supérieures à 3 mm, et à environ ±0,5 mm pour celles moins profondes.

* LRMP/CANMET
** Université d'Ottawa

INTRODUCTION

The AC potential drop technique is being used in the PMRL/CANMET project "Materials for Offshore Structures", to monitor the growth of fatigue cracks in welded plate T-joints (1). In the first phase of the project the effect of section thickness on fatigue life in the laboratory air environment has been investigated. In addition to multiprobe ACPD measurements, beach marking techniques were used to monitor the shape and size of growing cracks (2,3).

Four to seven beach marks were introduced in every specimen, either by ink staining, for the first beach mark, or by a temporary change in loading conditions, for subsequent beach marks. The beach marking revealed that a number of cracks, with an initial shape that is close to being semi-circular, start to grow from the weld toe. These cracks coalesce as they grow, forming fewer, larger semi-elliptical cracks, and eventually, after breaking through the plate edges, one almost straight-fronted crack. The number of initiated cracks and the resulting rate of transition to straight-fronted cracks (SFC) increases with applied stress range and plate thickness (2).

The ACPD measurements severely underestimate the depths of the initial semi-elliptical cracks if the standard calibration equation, based on AC current skin effect, is used (3). For tests in air, beach marks were used to calibrate ACPD measurements to obtain the maximum crack depth in the initial stages of fatigue crack growth.

In corrosion fatigue testing, beach marks cannot be produced. Instead, an ACPD calibration procedure based on empirical crack shape correction factors derived from measurements made in air was developed. The procedure is described in this report.

TEST WELDED JOINTS AND ACPD INSTRUMENTATION

The geometry and size of the welded test specimens used to examine the effects of section thickness on fatigue life in air and seawater environments is shown in Fig. 1. Details of fatigue test procedures are given in Ref. 3. The AC potential across a weld toe from where fatigue cracks initiate and grow, is monitored by eighteen spot welded probe pairs spaced 10 mm apart as shown in Fig. 1. Only two reference probe pairs located one quarter width distance from the edges, near active probes No. 5 and 15, are used.

The potential drop is measured by a crack-microgauge, Model U7G, manufactured by Unit Inspection Company (1). The potential signal from single probe pairs is fed into a microgauge through a 20 channel low voltage switching unit. The amplified DC signal from the microgauge is monitored by a computer. Fatigue testing is stopped periodically and the potential along the length of the weld is scanned. During the scan the cyclic load is held at a mean level.

The ACPD technique takes advantage of a skin effect. For a uniform current field and straight-fronted crack the crack depth a_p, can be calculated from Eq 1:

$$a_p = \frac{\Delta}{2} \left(\frac{V}{V_o} - 1\right) \tag{1}$$

where Δ = 10 mm is the probe length, V is the potential measured across the crack and V_o is the reference potential measured by reference probe pairs located next to the crack on the base plate.

For potential measurements in welded joints, one spot welded probe in the active pair sits on top of an irregular weld toe pass, and the surface distance Δ varies in single probe pairs; $\Delta = 10 \pm 1$ mm. Because of the variation in Δ and irregularities in potential field, the initial ratio of $\left(\frac{V}{V_o}\right)_{a=0}$ is not equal to one but varies from 0.85 to 1.40, with high values measured by probes closest to the plate edges. Equation 1 is modified to:

$$a_p = A \left[\left(\frac{V}{V_o}\right)_a - \left(\frac{V}{V_o}\right)_{a=0} \right] \tag{2}$$

where A is a calibration coefficient.

For tests in air, where four to seven crack depth measurements from beach marks were available for every specimen and probe location, the individual calibration curves, with variable coefficient A, can be obtained and used for converting potentials into crack depth (2,3).

For tests in seawater, only the final crack depth is available for calibration. The fatigue tests are terminated when the maximum crack depth reaches approximately one half the specimen thickness. After a test, the

specimen is fractured and the final crack depth under all probes is measured. For intermediate crack depth determination the following semi-empirical calibration procedure has been developed.

CRACK SHAPE CORRECTION FACTOR

Beach marks in individual air tests (2,3) indicate that a widely varying number of randomly distributed cracks start at the 203 mm long weld toe. Extreme examples - 3 cracks for a 26 mm thick specimen tested at a low stress range of 100 MPa, and 38 cracks for a 78 mm thick specimen tested at a high stress range of 200 MPa, are shown in Fig. 2a and 2b, respectively. Initial cracks tend to be clustered, and a rise in potential is detected also by probes located just outside the cracks. As a result, the potential distribution may indicate a cluster of cracks as one crack with a greatly underestimated maximum depth if Eq 2, with $A = \Delta/2$, is used. Examples of actual crack shape and distribution compared with potential drop measurements, taken from Ref. 3, are given in Fig. 3a, and 3b for 26 and 78 mm thick joints tested at 100 MPa stress range.

Because of the uncertainty in number and shape of cracks detected as one crack by potential distribution, the theoretical correction factors proposed for determining the depth of single semi-elliptical cracks (1) cannot be used. Instead, the crack shape correction factor, a_b/a_p is determined empirically. a_b is the maximum depth of a crack, as measured by a beach mark within a cluster indicated as one crack by potential distribution, and a_p is the crack depth determined from the maximum potential when inserted in Eq 2 with $A = 5$. The surface length of the crack (indicated by potential distribution) is, for convenience, defined by the number of probes straddled by the crack. The probe spacing is always 10 mm. The probes counted to be within the crack are those with potential readings higher than 30% of the central probe maximum potential reading. For example, in Fig. 3a, the first potential distribution at 2000 kc detects 2 cracks, of which one is actually two cracks straddling four probes (No. 6-9), and the second, one crack only straddling two probes (No. 12,13). The second potential distribution at 2800 kc indicates one crack where two exist straddling seven probes (No. 6-13).

The crack shape correction factors a_b/a_p, determined from air tests of nine specimens are plotted vs. number of probes n, in Fig. 4. The

power law best-fit curve shown in the figure, and defined by Eq 3 appears to fit the experimental data reasonably well:

$$\frac{a_b}{a_p} = 6.56(n)^{-0.6} \qquad (3)$$

CALIBRATION OF ACPD MEASUREMENTS

This calibration procedure determines the maximum depth of a dominant crack, i.e., the first crack to start, and initially the fastest growing, during a fatigue test of a welded joint. The calibration, performed by a computer program, consists of three steps:

1. From a printout of potential for each measurement, the number of cycles N_i at which the potential begins to increase steadily is selected for each probe. A mean value of all readings up to N_i is the $(\frac{V}{V_p})_{a=0}$ ratio in Eq 2. Next, the probe with the earliest, and initially the fastest increase in potential is identified.
2. For this probe, the initial calibration for a straight-fronted crack (SFC) is performed with Eq 2 with an A value determined from the final crack depth measurement and its corresponding potential reading. Because the final crack shape is still semi-elliptical in many tests, the value of A calculated is divided by an appropriate shape correction factor calculated with Eq 3 from probe readings within the crack (with potential readings higher than 30% of the maximum reading). Note from Fig. 4 that even for cracks spreading over all eighteen probes a small mean correction factor of 1.15 still applies.
3. SFC depths are calculated and corrected by an appropriate shape correction factor. Examples of calibrated crack depths measured on welded T-joints 26 and 78 mm thick, tested at stress ranges of 80, 100, 150 and 200 MPa in air, are shown in Fig. 5-11. The bottom curves are the calculated straight-fronted crack depths. After correction for shape, the crack depths, shown by diamonds, occasionally exhibit an apparent sudden drop, and the scatter is much wider than the scatter of SFC data. The apparent drops in crack depth are caused by a sudden increase in the number of probes straddled by a crack when two or more major cracks coalesce. To

avoid these apparent drops in crack depth, the crack shape correction factors were smoothed. The relationship of the correction factor to number of cycles is nearly linear. The best fit line extrapolated back through the test data from the measured values at the final crack depth, was used in calculating of the crack depth. These results, shown as triangles in Fig. 5-11, are compared with actual maximum crack depths, shown as stars, measured from beach marks.

DISCUSSION AND CONCLUSIONS

The aim of this ACPD calibration procedure is to determine the maximum depth of the largest fatigue crack, growing from the toe of a welded joint. Particular attention is paid to sizing the many initial cracks, because their growth and coalescence constitutes a major part of the fatigue life, and is little understood.

Calibrated maximum crack depths are compared with those measured from beach marks for a wide range of plate thicknesses and stress ranges in Fig. 5-11. It can be seen that for cracks deeper than 3 mm (approximately the depth of the first beach mark) the calibration error is within ±20%. The worst errors occur at intermediate crack depths, when cracks break through the plate edges, i.e., during transition from an embedded to a through-crack. For shallower cracks, a_{max} <3 mm, the error is difficult to assess. However, ±0.5 mm, which was the direct calibration error estimated from beach marks (2,3) seems to be appropriate. This supposition is supported by comparing of the first beach mark with the calibrated crack depths in Fig. 5-11.

The principal sources of error in calibrating crack depths are:

1. Variation in the number and shape of actual cracks detected as one crack by ACPD measurements. This variation is reflected in the value of crack shape correction factor, which as seen from Fig. 4 varies about the mean by a factor of ±2. Large correction factors apply when joints are tested at lower stress ranges where fewer cracks initiate and persist through most of the fatigue life as embedded semi-elliptical cracks. The errors associated with correction factors are proportional to their size. The best agreement between a calibrated and actual a_{max} is found with 78 mm thick plates tested at a 150 and 200 MPa stress range, Fig. 10, 11. Here, numerous initial cracks result in early coalescence into one straight-fronted crack, at a depth close to 5 mm.

2. Cracks at an irregular weld toe start in different planes. When mismatched cracks coalesce, the link (bridge) between two planes called line contact in (1) can remain unbroken until the crack becomes rather deep, and creates an electrical short circuit. Steps left by these links can be observed on the fractured surface, as shown in Fig. 2a. Line contacts can be numerous, and when major ones break, the potential measured by nearby probes increases abruptly. Thus, in this calibration procedure, line contacts can produce large errors in the apparent depth of intermediate crack.
3. Non-uniformity of potential across the width of a plate. As can be seen from Fig. 3, the potential measured by probes close to plate edges begins to increase very rapidly when an embedded crack starts to turn into a through crack. For a straight-fronted crack (Fig. 3b) the potential near the plate edges is higher than the potential at the plate center. Thus, near edge probes produce larger errors when calibrating cracks of intermediate depth than central probes. Luckily, in all specimens tested, cracks first started in the central part of the plate.
4. Fluctuations in potential measurements are responsible for perturbations in fatigue crack growth curves.

REFERENCES

1. Collins, R., Dover, W.D. and Michael, D.H. "The use of AC field measurements for nondestructive testing"; Nondestructive Testing Vol. 8, Academic Press Inc., London, 1985, pp. 211-267.

2. Vosikovsky, O., Bell, R., Burns, D.J. and Mohaupt, U.H. "Fracture mechanics assessment of fatigue life of welded plate T-joints including thickness effect"; Proceedings of BOSS Conference, Delft The Netherlands, Elsevier Science Publishers, July 1985, pp. 453-464.

3. Vosikovsky, O. and Rivard, A. "Effect of section thickness on fatigue life of welded plate T-joints", CANMET/PMRL Report 86-65(TR), Nov. 1985.

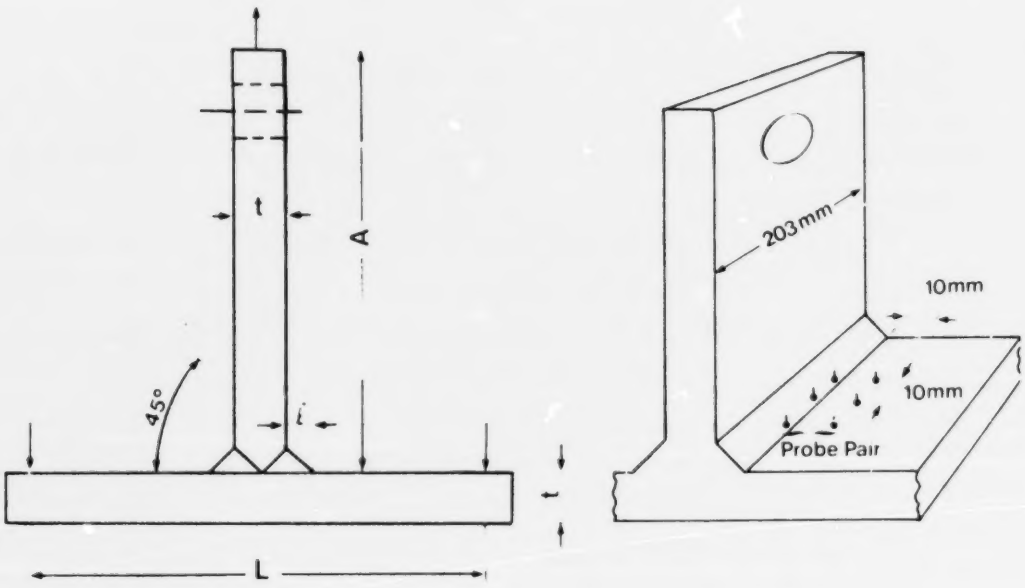

JOINT	t (mm)	ℓ (mm)	L (mm)	A (mm)
A	16	8-12	300	406
B	26	14-18	442	406
C	52	26-30	442	406
D	78	38-42	584	457
E	103	52-56	726	457

Fig. 1 - Geometry and dimension of tested welded plate T-joints, and location of ACPD probes

(a) t = 26 mm, $\Delta\sigma$ = 100 MPa

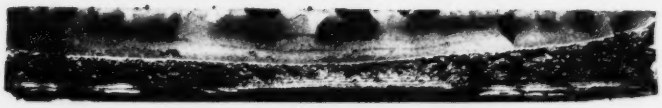

(b) t = 78 mm, $\Delta\sigma$ = 200 MPa

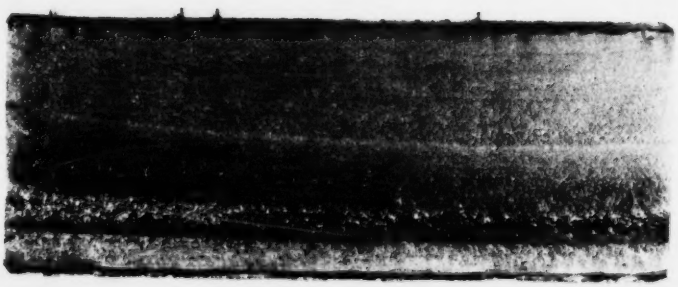

Fig. 2 - Examples of variation in number and shape of fatigue cracks with stress range and thickness

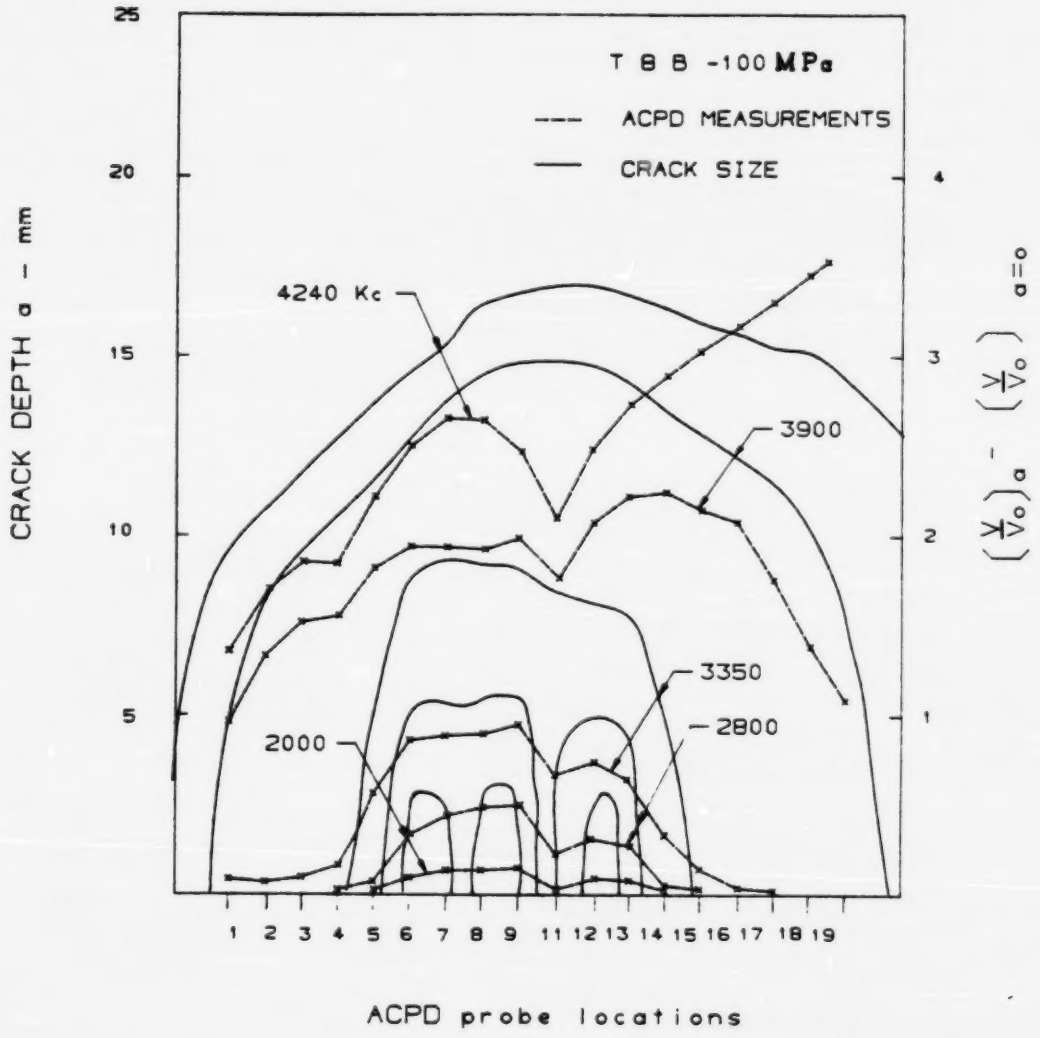

Fig. 3a - Comparison of crack depths calculated from ACPD measurements by Eq 2 with A = 5, with actual cracks size, measured from beach marks

t = 26 mm, $\Delta\sigma$ = 100 MPa

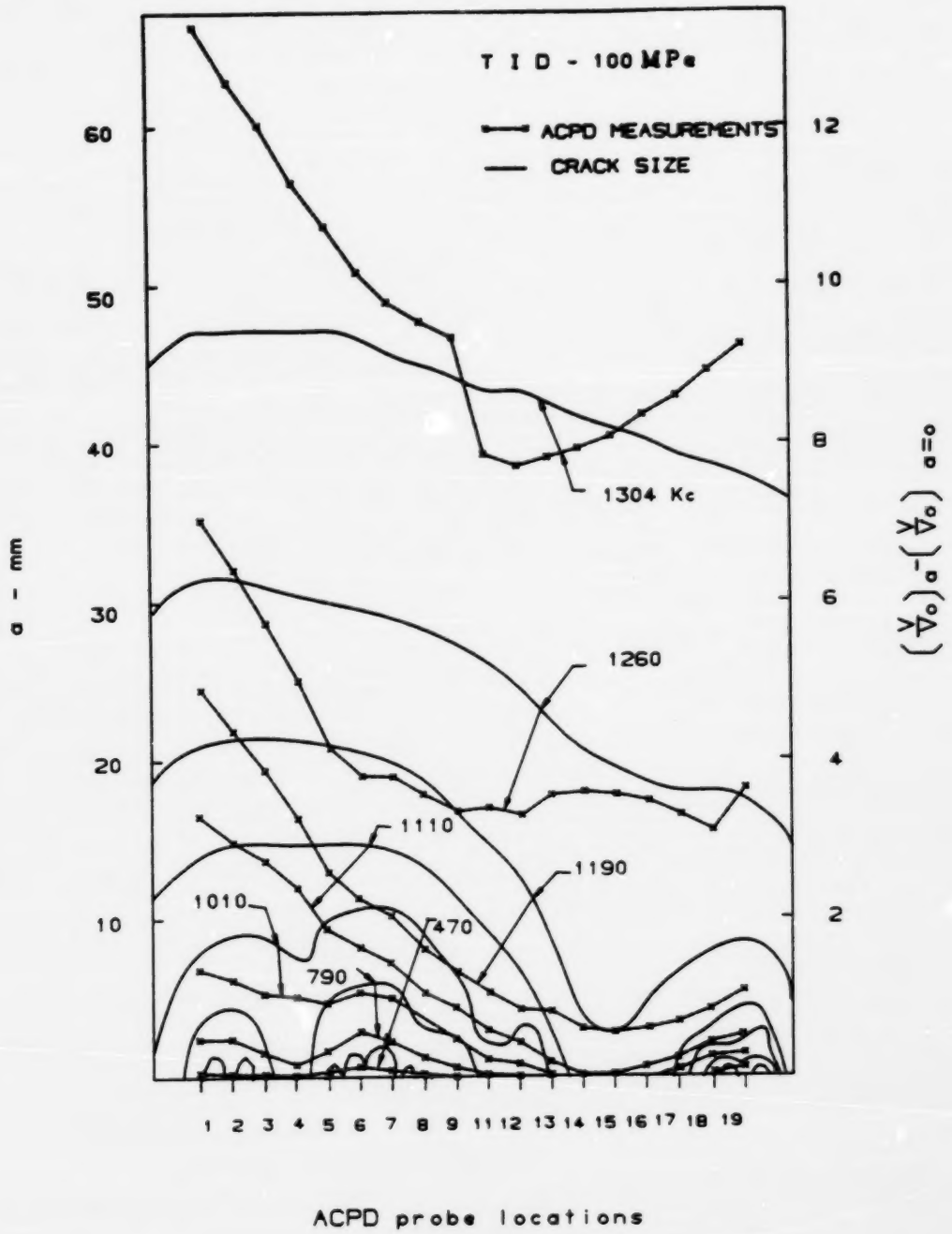

Fig. 3b - Comparison of crack depths calculated from ACPD measurements by Eq 2 with A = 5, with actual cracks size, measured from beach marks

t = 78 mm, $\Delta\sigma$ = 100 MPa

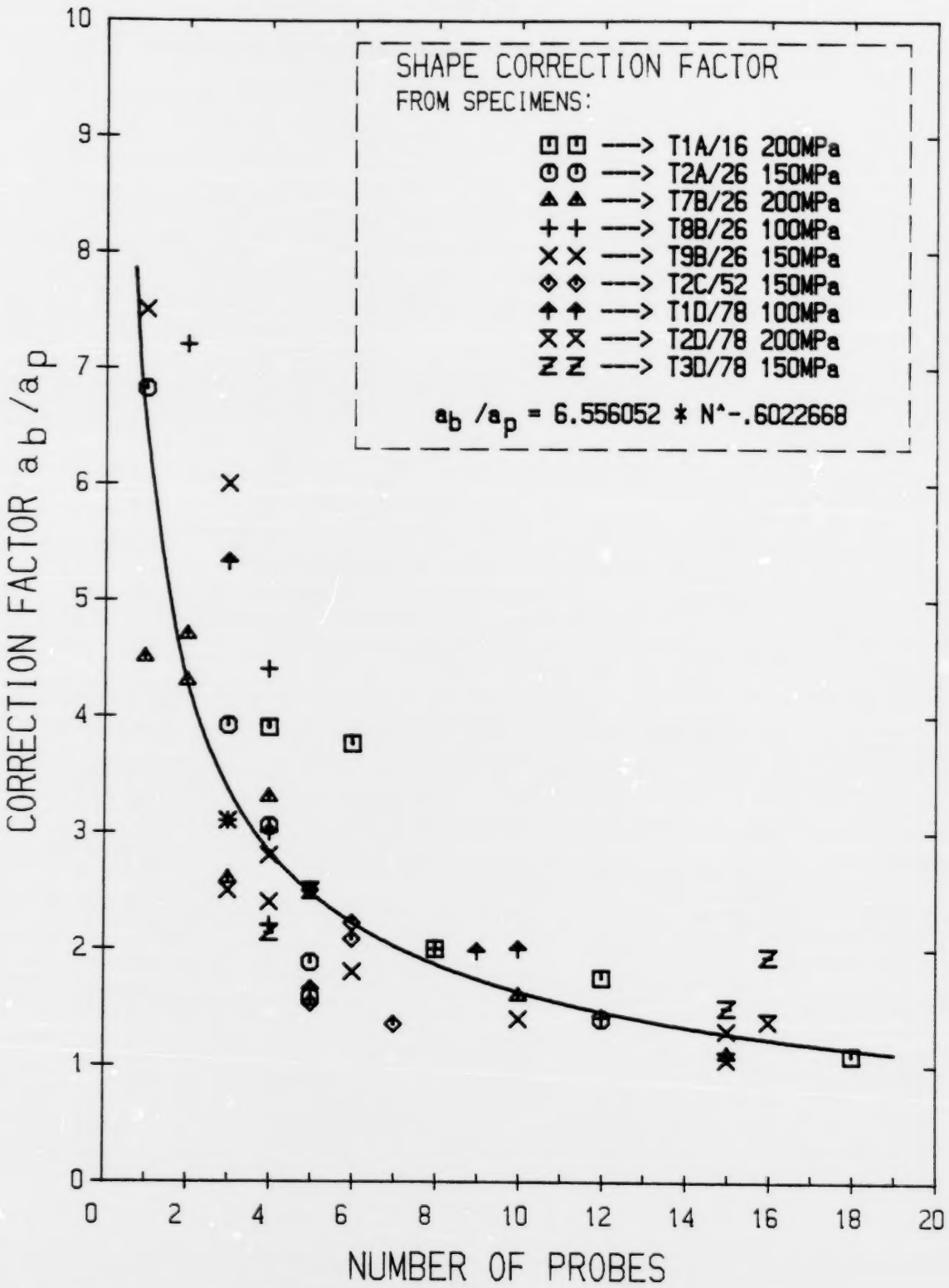

Fig. 4 - The dependence of crack shape correction factors on surface crack length, as defined by the number of probes straddled by the crack. Probe spacing is 10 mm. Data measured on twelve specimens are shown. The curve is the best fit regression curve.

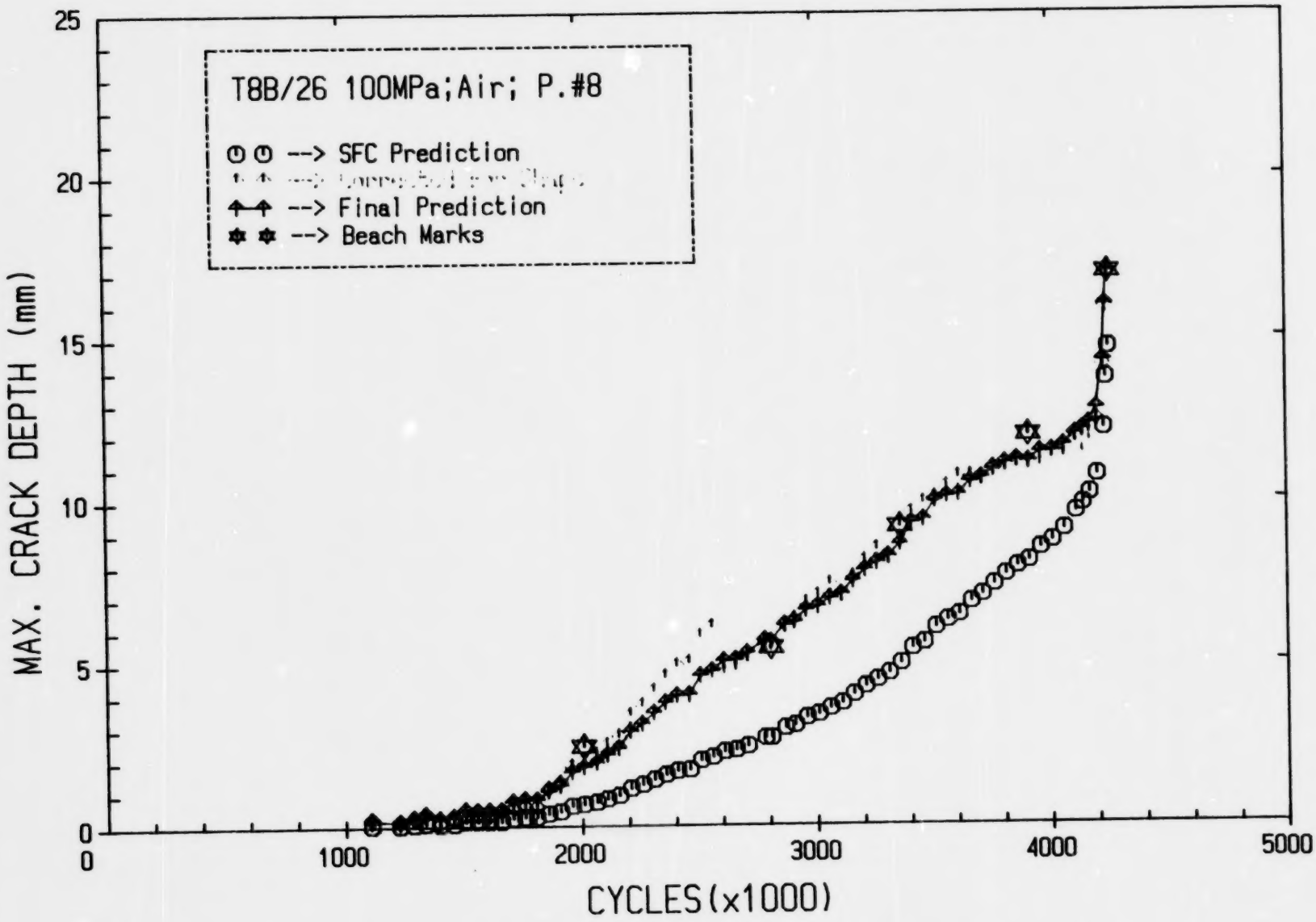

Fig. 5 - Maximum depths of a dominant fatigue crack determined from ACPD measurements for, a straight-fronted crack, a crack corrected for shape, and a crack corrected for shape by a smoothed correction factor. The actual maximum crack depths, measured from beach marks, are included for comparison. Specimen T8B, t = 26 mm, $\Delta\sigma$ = 100 MPa, probe No. 8.

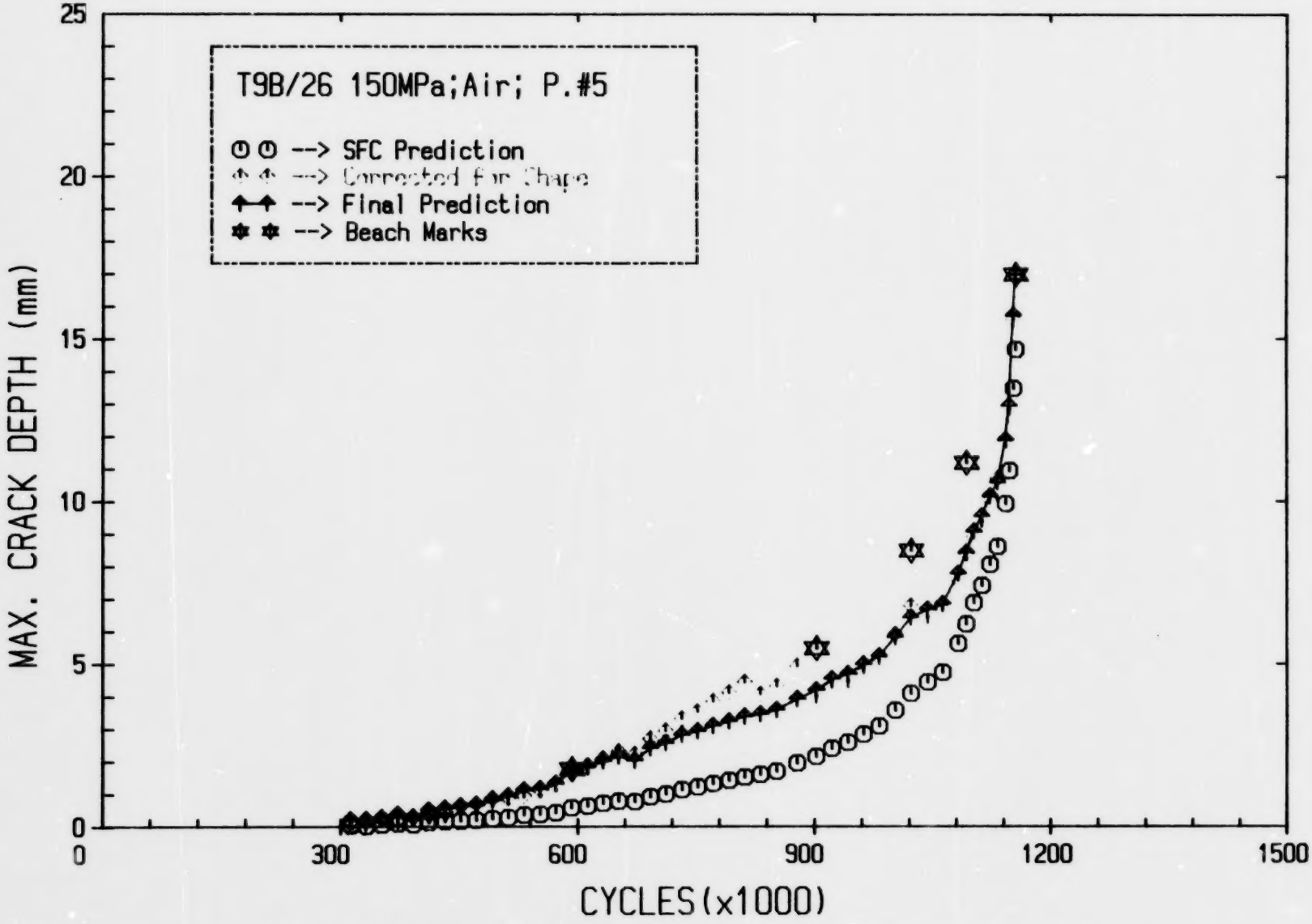

Fig. 6 - Maximum depths of a dominant fatigue crack determined from ACPD measurements for, a straight-fronted crack, a crack corrected for shape, and a crack corrected for shape with a smoothed correction factor. The actual maximum crack depths, measured from beach marks, are included for comparison. Specimen T9B, t = 26 mm, $\Delta\sigma$ = 150 MPa, probe No. 5.

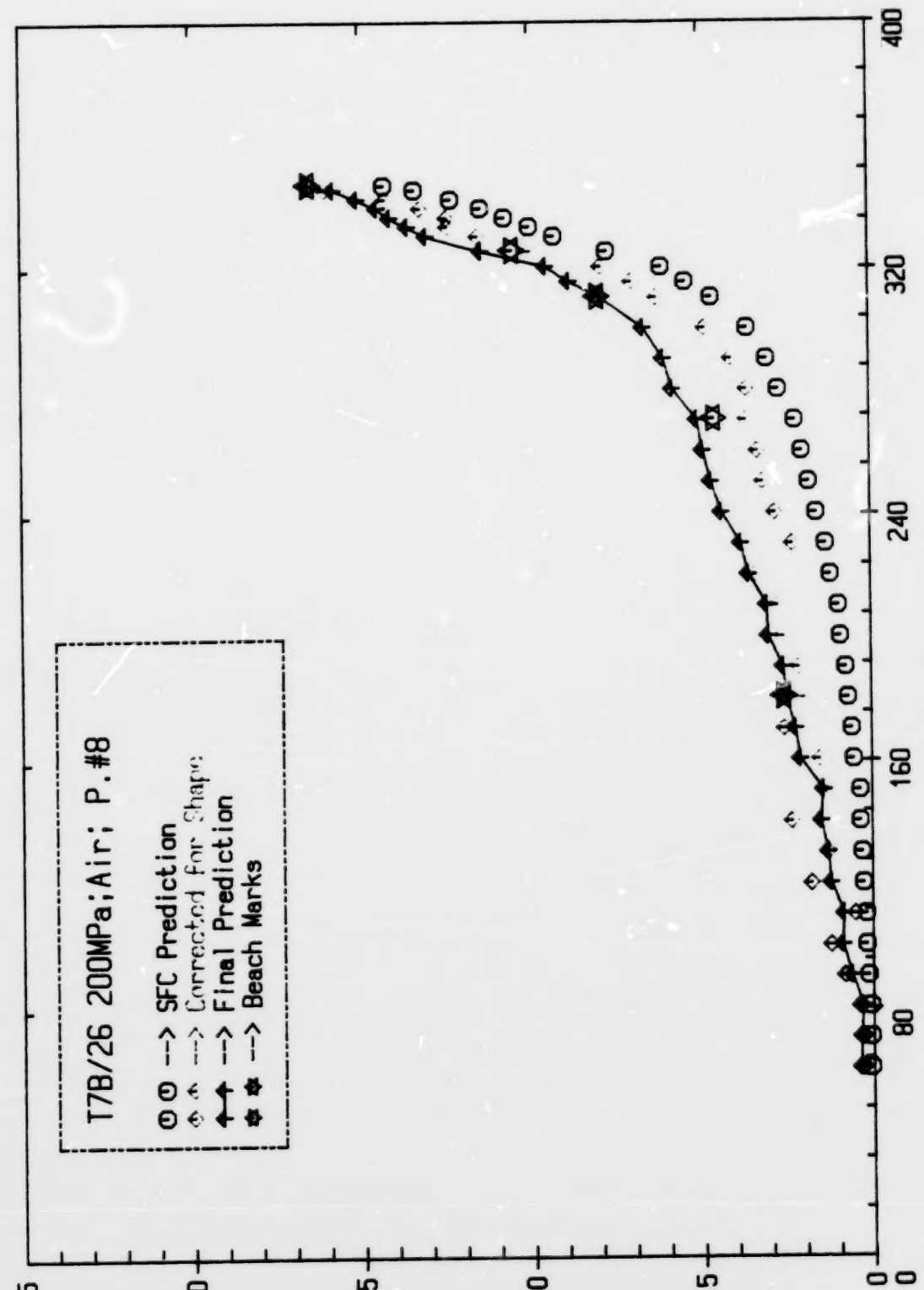

Fig. 7 - Maximum depths of a dominant fatigue crack determined from ACPD measurements for, a straight-fronted crack, a crack corrected for shape, and a crack corrected for shape with a smoothed correction factor. The actual maximum crack depths, measured from beach marks, are included for comparison. Specimen T7B, t = 26 mm, $\Delta\sigma$ = 200 MPa, probe No. 8.

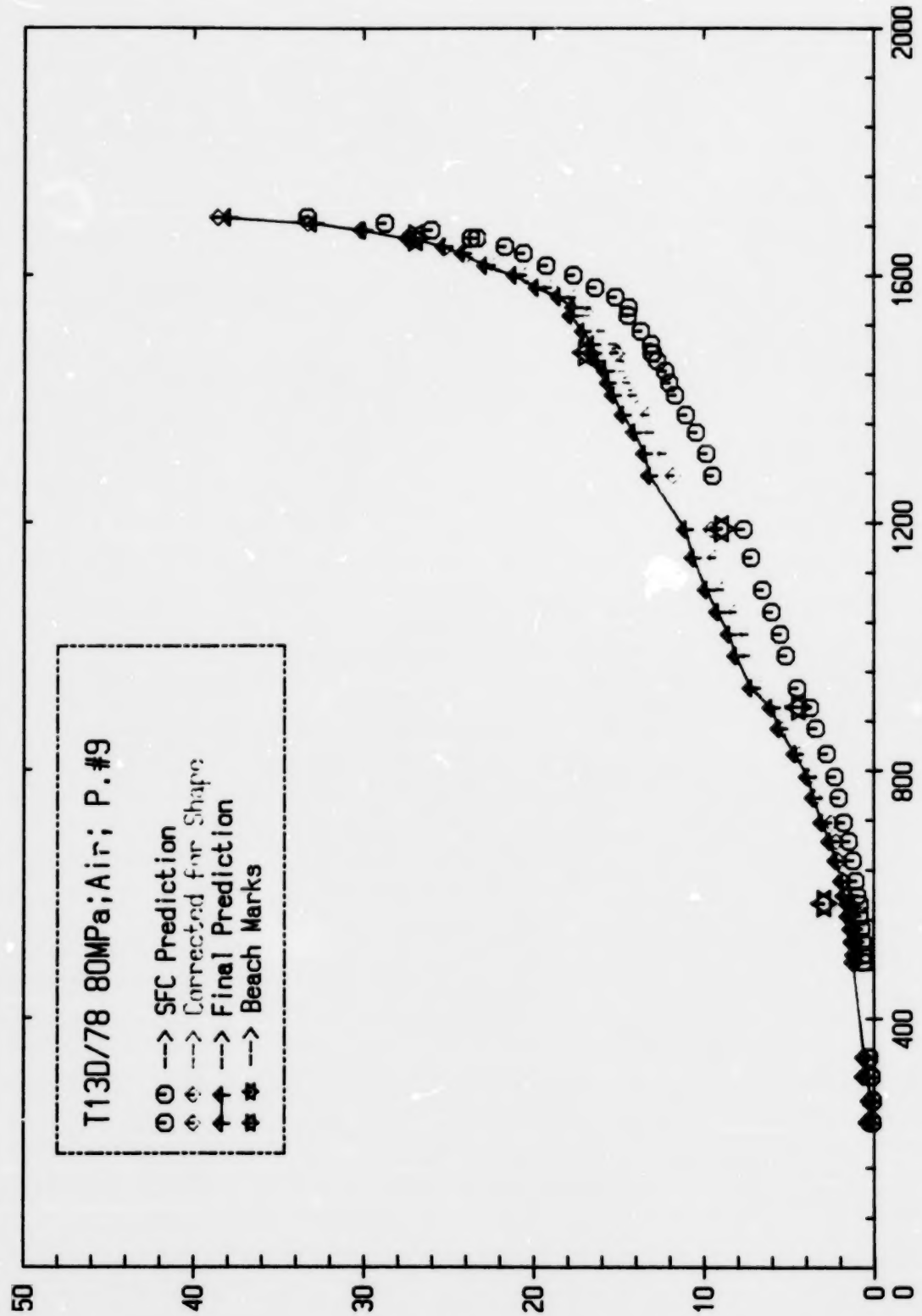

Fig. 8 - Maximum depths of a dominant fatigue crack determined from ACPD measurements for, a straight-fronted crack, a crack corrected for shape, and a crack corrected for shape with a smoothed correction factor. The actual maximum crack depths, measured from beach marks, are included for comparison. Specimen T13D, t = 78 mm, $\Delta\sigma$ = 80 MPa, probe No. 9.

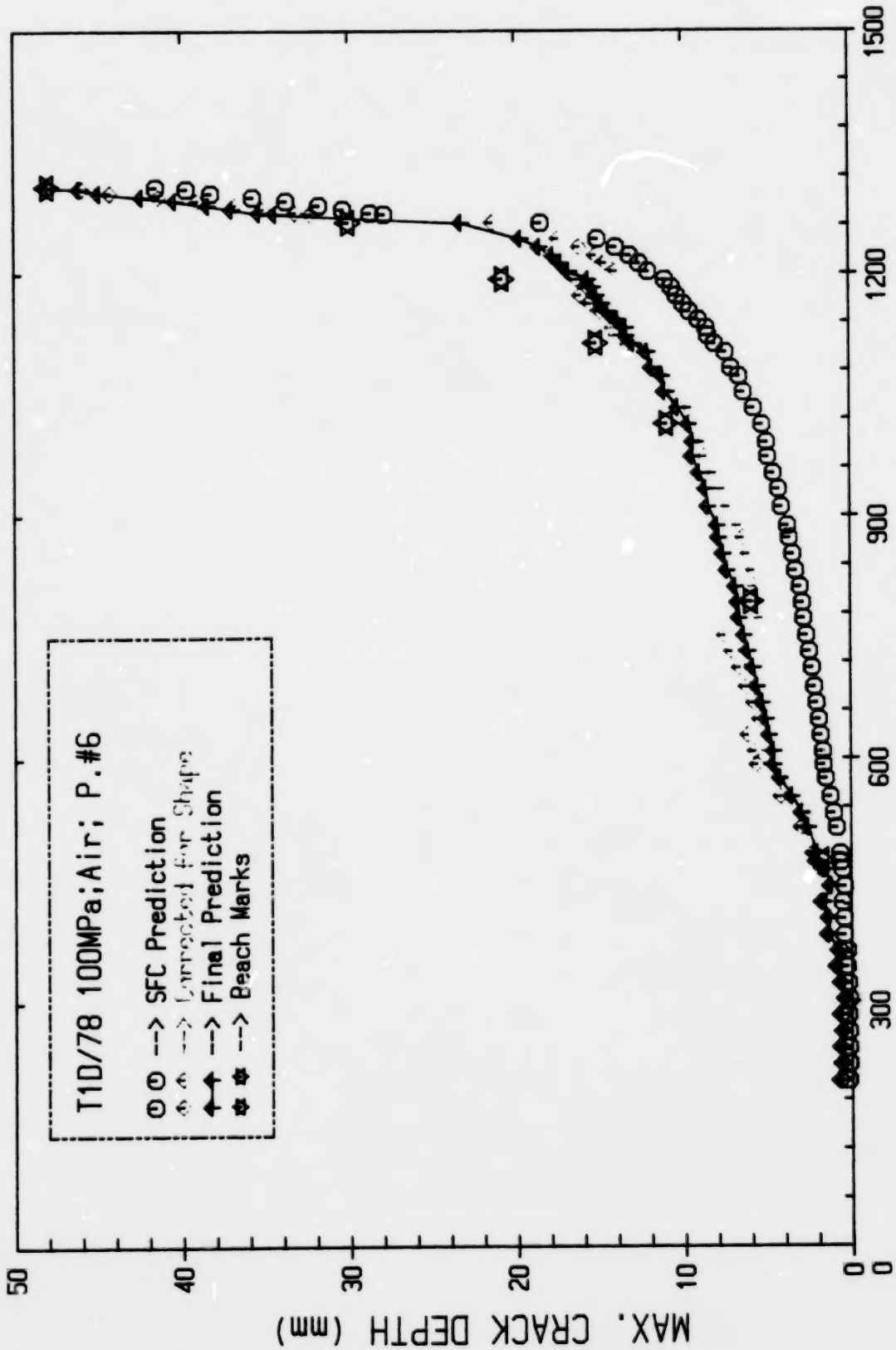

Fig. 9 - Maximum depths of a dominant fatigue crack determined from ACPD measurements for, a straight-fronted crack, a crack corrected for shape, and a crack corrected for shape with a smoothed correction factor. The actual maximum crack depths, measured from beach marks, are included for comparison. Specimen T1D, t = 78 mm, $\Delta\sigma$ = 100 MPa, probe No. 6.

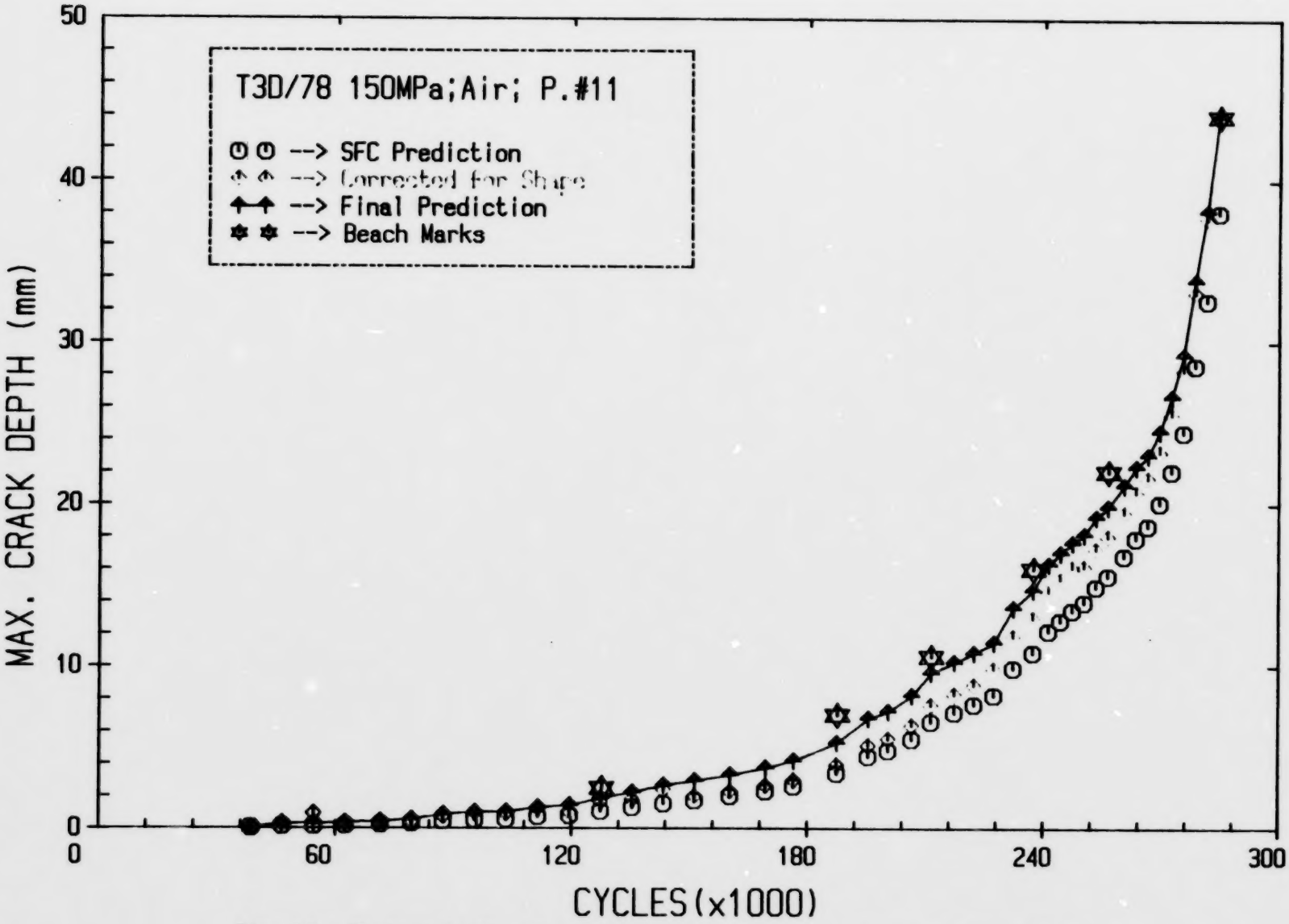

Fig. 10 - Maximum depths of a dominant fatigue crack determined from ACPD measurements for, a straight-fronted crack, a crack corrected for shape, and a crack corrected for shape with a smoothed correction factor. The actual maximum crack depths, measured from beach marks, are included for comparison. Specimen T3D, t = 78 mm, $\Delta\sigma$ = 150 MPa, probe No. 11.

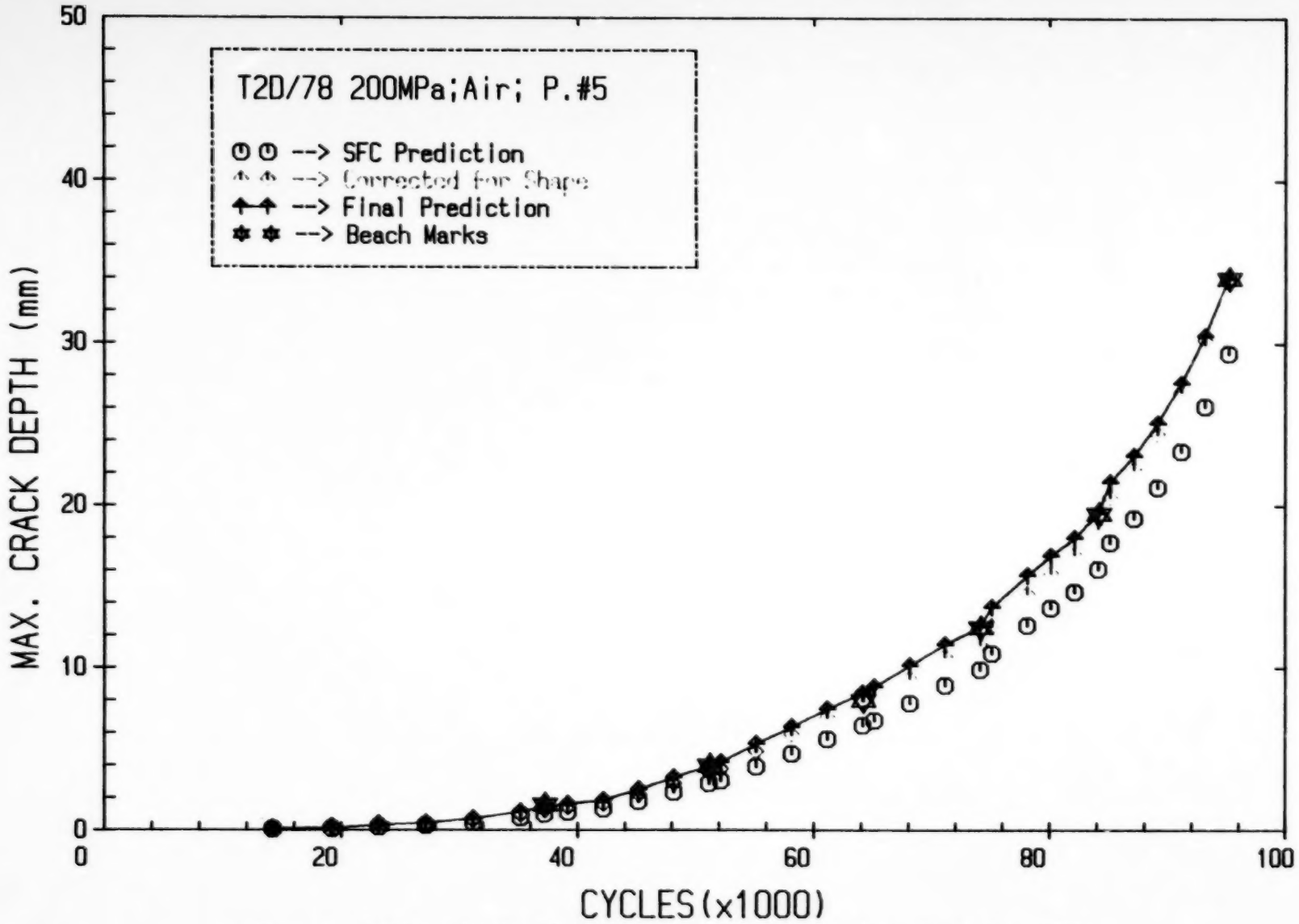

Fig. 11 - Maximum depths of a dominant fatigue crack determined from ACPD measurements for, a straight-fronted crack, a crack corrected for shape, and a crack corrected for shape with a smoothed correction factor. The actual maximum crack depths, measured from beach marks, are included for comparison. Specimen T2D, t = 78 mm, $\Delta\sigma$ = 200 MPa, probe No. 5.